Results in Surfaces and Interfaces 12 (2023) 100139

Contents lists available at ScienceDirect

Results in Surfaces and Interfaces

journal homepage: www.elsevier.com/locate/rsurfi

Enhanced corrosion protection of Cu & Al in Saline media using a new PEDOT based waterborne polyurethane coating

Raman Kumar [a,*], Swapnil S. Karade [a,b], Surendra K. Shinde [c], Swapnil K. Warkhade [d]

[a] Department of Chemical and Biomolecular Engineering, Yonsei University, 50 Yonsei-ro, Seodaemun-gu, 03722, Seoul, Republic of Korea
[b] Research Initiatives for Supra-materials, Shinshu University, Wakasato, Nagano, 380-0928, Japan
[c] Department of Physics, Arts, Science & Commerce College, Indapur, Pune 413106 Maharashtra, India
[d] Research and Quality Assurance, CSIR-Central Institute of Mining and Fuel Research Centre, Ranchi, Jharkhand, India

ARTICLE INFO

Keywords:
Corrosion
Impedance
Polarization
Coating
Graphene
PEDOT

ABSTRACT

In the present investigation, a new nanocomposite (PGZ) viz. PEDOT (poly(3,4-ethylenedioxythiophene)/ Graphene oxide (GO)/Zirconia (ZrO_2) has been developed via in-situ chemical oxidative polymerization method. Its electrochemical response as a preventive coating for inflating the corrosion resistance of industrial alloys i.e. copper (Cu) and aluminum (Al) exposed to neutral chloride (3.5% NaCl) environment at room temperature has been analyzed using various electrochemical techniques. Both the substrates along with the nanocomposite material (PGZ) have been characterized by various surface analysis studies viz. FE-SEM, XRD, TGA, TEM, EDAX and FT-IR studies. The SEM studies showed the compact formation of coating on the substrate. Other characterization studies well established the formation of PGZ nanocomposite. The experimental electrochemical investigations on coated substrates demonstrated a significant reduction in the corrosion current density (i_{corr}) and a fascinating increase in the charge transfer resistance (R_{ct}) values in comparison to the bare metal specimens.

1. Introduction

Corrosion of industrial alloys specifically copper (Cu) and aluminum (Al) is a subject of huge concern for various industries. Their gradual depletion after coming in contact with the aggressive environment, during various industrial processes results in enormous economic loss of both direct and indirect type (Liu et al., 2015; Lokesh et al., 2012; Rickerby and Steinke, 2002; Liu et al., 2016; Kinsella et al., 2003; Lamaka et al., 2007; Zhao et al., 2001). The extensive use of aggressive electrolytes in these industrial processes triggers the destructive electrochemical corrosion reactions on the surface of these important metals (Steppan et al., 1987; Fenelon and Breslin, 2002; Cascalheira et al., 2003; Brusic et al., 1997; Beccaria and Chiaruttini, 1999). Several strategies including the use of cathodic/anodic protection (Kear et al., 2005; Li et al., 2018; Simões et al., 2007; Cecchetto et al., 2007), inhibitors (Fateh et al., 2017; Xhanari and Finšgar, 2016), paints, coatings (Kowalczyk and Luczka, 2015; Stankiewicz et al., 2013) etc. have been adopted to minimize this destructive force of corrosion. Among all these methods the most convenient and promising way to combat corrosion is the use of barrier coatings. Chromate-based anti-corrosion coatings are proven to be very effective but their toxic nature is a huge drawback for the concerned industries (Kendig et al., 1993; Bastos et al., 2005; Shi and Dalal, 1994). The organic/inorganic nanocomposite coatings comprising of sustainable components are the ideal substitute for these chromate based coating materials, which provides significant corrosion deterrence for a prolonged period of time (Nguyen-Tri et al., 2018).

Several researchers have reported the use of polymeric nanomaterials as anti-corrosion coating, R. Hasanov et al. (Hasanov and Bilgiç, 2009) explored the use of monolayer and bilayer polymer coatings, including polypyrrole (PPY) and polyaniline (PANI), on steel electrodes for corrosion protection. The coatings were deposited via electro-polymerization in oxalic acid solution, and their effectiveness in inhibiting corrosion was evaluated in 1 M H_2SO_4 solution. The study found that the bilayer coatings showed better corrosion inhibition than the monolayer coatings, with PPY/PANI offering the highest level of protection. The coatings were characterized by FTIR spectroscopy and SEM. C.K. Tan et al. (Tan and Blackwood, 2003) investigated the effectiveness of multilayered coatings consisting of polyaniline (PANI) and polypyrrole (Ppy) in providing a barrier against corrosion in chloride environments. The coatings were galvanostatically deposited on carbon steel and stainless steel, and their performance was evaluated using potentiodynamic polarization. The results showed that the multilayered coatings were significantly better at protecting against pitting corrosion than single Pani coatings on stainless steel, with films consisting of

* Corresponding authors.
E-mail addresses: raman20788@gmail.com (R. Kumar), karadeswapnil18@gmail.com (S.S. Karade).

https://doi.org/10.1016/j.rsurfi.2023.100139
Received 27 March 2023; Received in revised form 1 August 2023; Accepted 1 August 2023

2666-8459/© 2023 The Author(s). Published by Elsevier B.V. This is an open access article under the CC BY-NC-ND license (http://creativecommons.org/licenses/by-nc-nd/4.0/).

a PANI layer over a Ppy layer yielding the best results. The study suggested that the ability of the conducting polymer film to act as electronic and chemical barriers was more important than its ability to act as a physical barrier in providing corrosion protection. J. E. Pereira da Silva et al. (da Silva et al., 2005) studied the use of a polymeric blend consisting of camphorsulphonate or phenylphosphonate-doped polyaniline (PANI) and poly(methyl methacrylate) for iron corrosion protection in sulfuric acid solutions with or without chloride ions. The study found that the blends act by a two-step protection mechanism involving a redox reaction between Fe and PANI leading to anion release, followed by the formation of a passivating complex between iron cations and the PANI doping anion, which acts as a physical barrier to prevent the penetration of aggressive ions. The study concluded that PANI can function as an anion reservoir and release anions in a smart way to protect the surface of the coating from damage. Kalendová et al. (2015) investigated the effect of conducting polymers and conducting pigments on the corrosion-inhibiting properties of zinc-filled organic coatings. The coatings containing carbon nanotubes and graphite coated with polypyrrole were found to be the most efficient in inhibiting corrosion. The conducting polymers also improved the coatings' mechanical properties. Hasanov et al. (2011) investigated the effects of poly(N-ethylaniline) (PNEA) monolayer coating and PPY/PNEA and PNEA/PPY bilayer coatings on the corrosion of low carbon steel (LCS) in 1 M H_2SO_4 medium. The coatings were formed via electropolymerization in a monomer and oxalic acid medium. The results showed that the coated LCS electrodes prevented corrosion in 1 M H_2SO_4 medium, and the bilayer coatings were more effective than the monolayer coating. The study also included theoretical calculations using the AM1 semiempirical method to better understand the interaction between the coatings and the metal. The calculated data supported the experimental findings.

The fabrication of sustainable coating materials involving suitable filler materials is anticipated to offer significant corrosion protection to metals exposed to highly aggressive environments. These coatings do not have any adverse effect on our eco-system. Their mode of action involves the entire/partial restoration of the defects via the polymerization of chemical species, trailed by mitigation of corrosion onset at the coating/metal interface (Nguyen-Tri et al., 2018).

A special class of conducting organic polymers viz. poly(3,4-ethylenedioxythiophene) (PEDOT), polythiophene, polypyrrole, polyaniline possess significant corrosion prevention characteristics when used as coatings materials (Bai et al., 2015). The dual defense system of these polymers delivers high-end corrosion protection to the coated metal substrates. The substantial barrier characteristics via developing a well adherent and highly compact protective film on the metal substrates and having the capacity to self-restoring small pores/defects resulted from prolonged exposure to the aggressive medium via forming metal/ion complexes at the metal/coating interface distinguish these polymers from other coating materials (Armelin et al., 2009).

The proficiency of these conducting polymers can easily be tailored by using different filler materials of choice to combat corrosion in a very effective manner. The main features which an ideal coating material should comprise of are the compact nature of the coating film, high wear resistance, high thermal and chemical stability and sustainable nature (Dutta and De, 2007; Shi et al., 2009). The current investigation is a compilation of various analyses performed on the newly developed PEDOT/Graphene oxide/ZrO_2 nanocomposite (PGZ), as a coating material for Cu and Al substrates subjected to 3.5% sodium chloride solution. This nanocomposite has been conveniently developed at −2.0 °C temperature via in-situ chemical oxidative polymerization method using appropriate solvents and reagents. Graphene oxide (GO) and zirconia (ZrO_2) have been used as filler materials, the former comprises of a hexagonal carbon web with sp^2 and sp^3 hybridized carbons with hydroxyl (–OH) groups, epoxide (–O–) linkages on its basal plane and carbonyl (–C=O) and carboxy (HO–C=O) groups at the boundaries. The functional groups having oxygen contributes towards the hydrophilic nature of GO, which also makes it easily dispersible in water and polymers. It has been widely publicized that GO is a promising strengthening agent for the nanocomposite protective coatings. It increases the stiffness, strength and its high surface area aids towards prohibiting diffusion of aggressive ions towards the metal surface (Lerf et al., 1998; Eda and Chhowalla, 2010; Stankovich et al., 2006; Putz et al., 2010; May et al., 2012; Padawer and Beecher, 1970; Cano et al., 2013). The later one i.e. ZrO_2 nanoparticles provide enhanced thermal stability and upsurge overall mechanical strength of the coating material (Muller et al., 2016). Water based polyurethane (WBPU) was used as a binder material in our study, as it also provides the much needed hydrophobicity (Christopher et al., 2016) to the overall coating formulation. Five different coating variants were prepared by homogenizing 1.0 to 5.0% of the composite material into the binder solution, subsequently, these formulations were uniformly brush coated onto the Cu and Al substrates. The effect of aggressive environment on these coated substrates have been elucidated in details using potentiodynamic polarization and electrochemical impedance spectroscopy (EIS). The endurance of this coating material has been tested for a period of up to 30 days. The main purpose of the present research work is to provide a new sustainable coating material, which can be reproduced easily via a simple method and provide significantly prolonged corrosion protection to the metals persistently subjected to the harsh environment.

2. Experiment

2.1. Materials

3,4-Ethylenedioxythiophene (EDOT), Dodecylbenzene sulfonic acid (DBSA), ammonium persulphate (APS), zirconia (ZrO_2) having particle size < 100 nm were purchased from Sigma Aldrich. Graphene oxide (GO) was acquired from Graphene Supermarket and polyurethane (WBPU) was acquired from Alberdingk-Boley. Double deionized water (specific resistivity of 10^6 Ω cm^2) was used to prepare aqueous solutions.

2.2. Fabrication of PEDOT/GO/ZrO_2 (PGZ) nanocomposite

In a 500 mL beaker, 0.2 M DBSA was homogenized with double deionized (DI) water for 1 h. Subsequently, 0.1 M EDOT, 10% GO and 20% ZrO_2 (Wt.% w.r.t. to EDOT) were added to the beaker and again homogenized for 1 h. The temperature of the beaker was maintained at −2.0 °C (±0.02 °C) using a refrigerated circulator (JEIO TECH, Model: VTRC-620) and 0.1 M APS solution was added dropwise to it with continuous stirring. The contents of the beaker were kept on vigorous mechanical stirring for next 8 h. The bluish black precipitates obtained were demulsified using isopropyl alcohol (IPA) and which were washed with doubly ionized H_2O till a pH in the range of 5–6 was achieved. The filtered precipitates obtained were kept at 60 °C overnight for drying.

2.3. Instrumentation

X-ray diffraction (XRD) data were recorded on Miniflex-Rigaku, Japan. The samples were scanned in a range between 5° to 80° at a scan rate of 2° per minute. SEM micrographs and corresponding EDAX profiling were recorded on FE-SEM, Model: JEOL-7800F Prime. TEM analysis and corresponding EDAX profiling has been carried out on a Transmission electron microscope, Model: JEOL-JEM (F200). FT-IR analysis was performed on Bruker FT-IR Spectrometer, Model: Vertex 70. The spectrums were recorded in transmittance mode between 400 cm^{-1} to 4000 cm^{-1}.

Electrochemical studies were performed on a high precision Biologic Instrument, Model: VSP/VMP3. The experiments were executed in a three-electrode assembly using standard calomel electrode (SCE) as a reference, platinum (Pt) wire as a counter electrode, Cu and Al specimens (dimensions: 1.5 cm × 1.5 cm × 0.1 cm) as working electrodes.

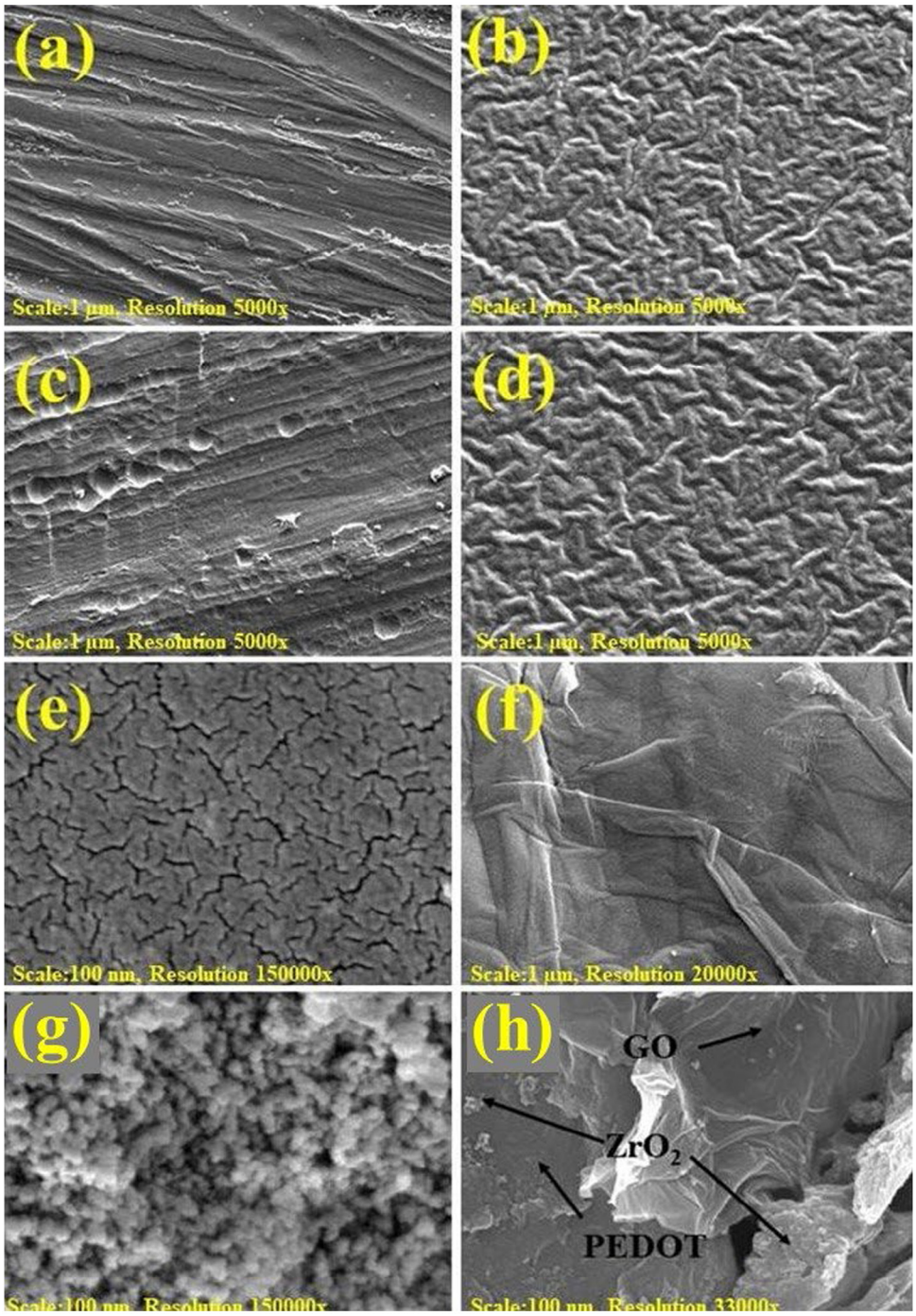

Fig. 1. FE-SEM micrographs of (a) bare Cu, (b) coated Cu, (c) bare Al, (d) coated Al, (e) PEDOT, (f) GO, (g) ZrO_2 nanoparticles and (h) PGZ nanocomposite.

The electrochemical impedance spectroscopy (EIS) was performed via administering a potential of 10 mV magnitude to the investigated system and subsequently scanning it in a frequency range of 100 KHz to 0.1 Hz. The impedance plots were analyzed using ZFit EC-Lab software and corresponding electrical circuits were proposed. Using these modeled circuits various impedance parameters were determined. Potentiodynamic/galvanostatic polarization parameters were recorded via sweeping the investigated coating system in the potential range of ±250 mV vs SCE (standard calomel electrode) at a scan rate of 1.0 mV s^{-1}.

3. Results and discussion

3.1. Morphological analysis of metal specimens and PGZ nanocomposite

Figs. 1a and 1c depict the corresponding SEM images of bare Cu and Al specimens. The uniform and homogeneous nature of the PGZ coating in WBPU over Cu and Al substrates can be observed from the Figs. 1b and 1d respectively. This SEM analysis shows the compact morphology of the coating material over the metal substrates. Fig. 1h presents the SEM micrographs of the PGZ nanocomposite.

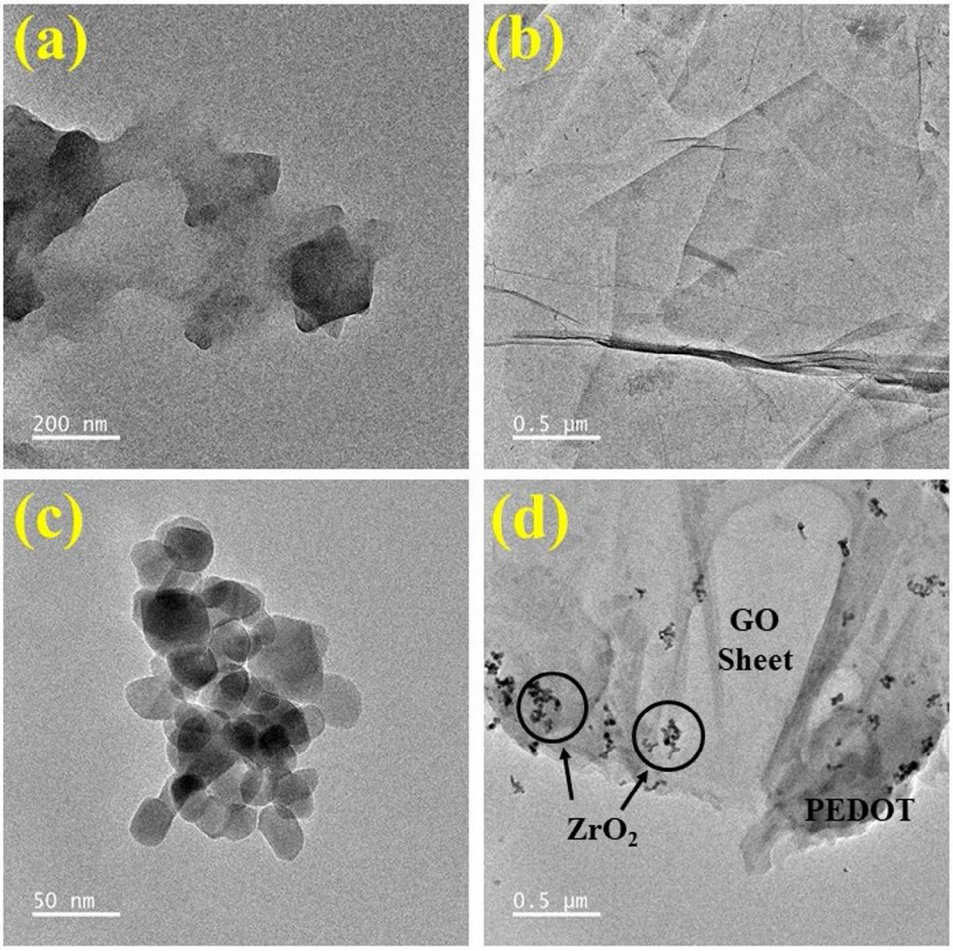

Fig. 2. TEM images of (a) PEDOT, (b) GO, (c) ZrO_2 nanoparticles and (d) PGZ nanocomposite.

The SEM image of PEDOT (Fig. 1e) illustrated an amorphous surface characteristic of this conducting polymer. The SEM profile of PGZ nanocomposite depicts a distinct modification on the surface features of polymer (PEDOT), which is attributed to the manifestation of GO sheet and ZrO_2 nanoparticles on the polymer grid. The SEM micrographs confirm PEDOT embedded with GO sheets and zirconia nanoparticles composite formation. The SEM images for GO and ZrO_2 nanoparticles are shown in Figs. 1f and 1g respectively. Fig. 2d shows the TEM image of GO sheets and ZrO_2 nanoparticles entrenched around the conducting PEDOT template. Fig. 2d also illustrates the presence of polymeric granular blots accumulated around GO sheets and ZrO_2 nanoparticles. The TEM images for PEDOT, GO sheet and ZrO_2 nanoparticles are shown in Figs. 2a to 2c correspondingly. The EDAX profile along with corresponding micrographs for PGZ nanocomposites have been shown in Fig. 3 along with elemental composition. It depicts the homogeneous blend of all the three components in the PGZ nanocomposite.

3.2. FT-IR investigations

Fig. 4 shows the FT-IR spectrum of PGZ nanocomposite, PEDOT and GO. The band observed at 1518 cm^{-1} is because of the C–C or C=C stretching vibrations. The C-O-C bond stretching in the ethylene dioxy group shows vibrational bands around 1204 cm^{-1}, 1141 cm^{-1} and 1050 cm^{-1}. The FT-IR signals at 980 cm^{-1} and 833 cm^{-1} attributed to the modes of deformation in the C–S–C bond of thiophene ring. The specific characterizing peak for the conducting polymer (PEDOT) was observed around 1340 cm^{-1} (Choi et al., 2004). The FT-IR investigation of GO shows its characteristic peaks for C–O, C–OH, C=O and –OH around 1047 cm^{-1}, 1579 cm^{-1}, 1720 $cm^{-1,}$ and 3430 cm^{-1} respectively (Rattana et al., 2012). The FT-IR spectrum of PGZ nanocomposite depicts entire vibrational bands as recorded for the PEDOT sample. Due to the weak interaction between GO and PEDOT the shifting of signals was observed which is further attributed to the wrapping or capping of PEDOT over GO sheets. As no new peaks were observed in the spectrum of PEDOT, it is inferred that there is no chemical interaction occurred between the GO and conducting polymer (PEDOT).

3.3. X-ray diffraction (XRD) studies

Fig. 5 shows XRD pattern for the as prepared PGZ sample with a supporting reference of ZrO_2 (JCPDS file 00-005-0543). Almost all the characteristic peaks of monoclinic ZrO_2 are perfectly coincides with the ZrO_2 sample. Further the peak at appeared at 10.5° for the sample bare GO corresponds to (001) plane which indicates a characteristic peak of graphite oxide. Moreover, the bare PEDOT samples shows broad diffraction peak at 25.8° corresponds to (020) plane confirms the complete polymerization of EDOT. Thus, the composite PGZ sample shows a combination of all peaks implies the successful chemical mixing of GO/ZrO_2 along with polymerization of EDOT to form an PGZ composite.

3.4. Thermogravimetric analysis (TGA)

Fig. 6 represents thermogravimetric analysis of PGZ sample. It reveals mass loss profile in two steps. In a first step the mass loss initiates at 60 °C and it is continuing up to 85 °C which is mainly due to removal of moisture present in the sample as well as low temperature

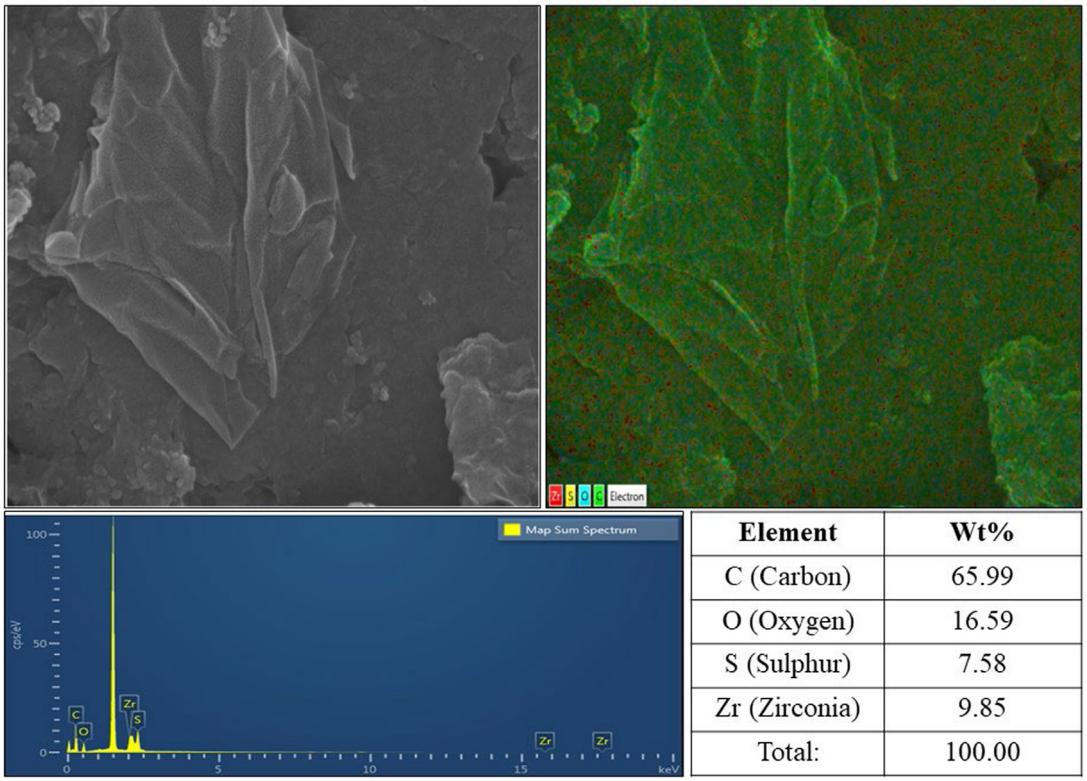

Element	Wt%
C (Carbon)	65.99
O (Oxygen)	16.59
S (Sulphur)	7.58
Zr (Zirconia)	9.85
Total:	100.00

Fig. 3. EDAX profile of PGZ nanocomposite.

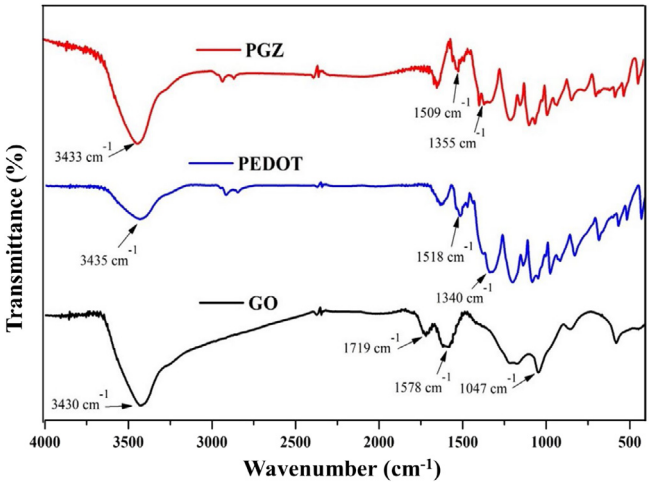

Fig. 4. FT-IR spectrums of PGZ, PEDOT and GO.

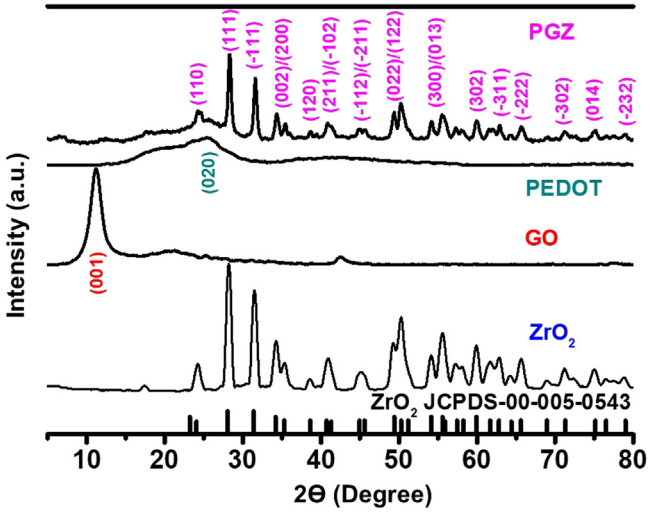

Fig. 5. XRD spectrums of PGZ, PEDOT, ZrO_2 nanoparticles and GO.

stability of graphene oxide (GO) (Kuila et al., 2013). The second mass drop is observed from 450 °C because of a break in the structure of the polymer chain in PEDOT (Khasim et al., 2021). Further increase in temperature initiates the loss of mass, depicted as linear region which further indicates that the PGZ composite structure is more stable in the range of 85 °C to 450 °C. Comparable temperature dependency is observed in the case of polymer doped metal oxide structure (PEDOT: PSS doped TiO2) (Khasim et al., 2021).

3.5. Impedance analysis of coated metal

Electrochemical Impedance Spectroscopy (EIS) is a powerful analytical technique used to investigate the electrochemical behavior of materials, including coated metals. EIS is particularly useful for studying the protective properties of coatings as it provides information on the coating's resistance to corrosion and its ability to impede the movement of ions through the coating. In an EIS study of coated substrate, a small AC voltage is applied to the coated sample, and the resulting current is measured as a function of frequency. The impedance of the coated sample is then calculated from the measured current and voltage data.

The impedance data obtained from EIS studies can be used to determine the protective properties of the coating, including its electrical resistance, capacitance, and charge transfer resistance. These parameters provide valuable information on the coating's ability to

Table 1
Charge transfer resistance (R_{ct}) values of bare metals (Cu and Al), WBPU coated metals and 3.0% PGZ in WBPU coated metals specimen exposed to 3.5% NaCl Solution.

Composition (%)	Charge transfer resistance (R_{ct}) Ω cm^2					
	After 1 day	After 5 days	After 10 days	After 15 days	After 20 days	After 30 days
For Copper (Cu) Specimens						
Bare Cu	8284	5286	4172	2407	1786	1493
WBPU	22277	20695	18790	12874	8303	12283
3.0% PGZ in WBPU	2.291×10^6	322508	29739	27827	28104	27141
For Aluminum (Al) Specimens						
Bare Al	285.5	425.9	264.3	101.4	41.17	23.4
WBPU	3356	3208	3061	2406	1570	956.2
3.0% PGZ in WBPU	157370	76018	21237	18278	16841	10074

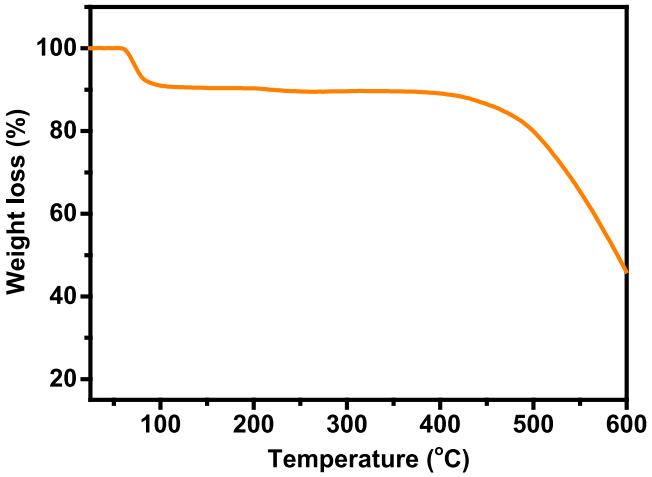

Fig. 6. TGA profile for the PGZ nanocomposite.

prevent the penetration of corrosive species, such as water and salts, into the underlying metal.

The bare and coated samples were kept in a 3.5% NaCl solution for a period of up to 30 days to check the durability and reliability of the coating material. Impedance spectroscopy (EIS) is a well-established non-detrimental electrochemical method accepted widely for the assessment of corrosion resistance offered by the coatings to the underlying substrates. These evaluations were performed via putting the WBPU (binder) coated Cu and Al substrates and WBPU with various loadings of PGZ nanocomposite (1.0% to 5.0%) coated substrates in 3.5% neutral chloride solution at steady state potential for a exposure period of 1 day to 30 days at 25 ± 2 °C (room temperature). The optimized concentration of 3.0% PGZ in WBPU demonstrates the most significant corrosion protection characteristics among all the other loading concentration of PGZ. The corresponding Nyquist and Bode's plots for Cu and Al specimens coated with the optimized concentration i.e., 3.0% of PGZ in WBPU after 1 day of exposure to the aggressive NaCl solution are displayed in Figs. 7 and 8 respectively.

The investigated system shows capacitive and resistive behavior as exhibited by one-time constant in the Nyquist plots; the observed impedance response was significantly high. A basic electrical circuit as shown in the fig. S5 in supplementary information, comprises of parallel coupled capacitor and resistor connected to a resistor in series was used to model the experimental data which yielded vital impedance parameters viz. charge transfer resistance (R_{ct}) and capacitance of the coating (C_c). R_{ct} signifies the corrosion resistance provided by the coating to the underlying metal substrates. C_c is another vital parameter which evaluates the reliability of coating material and also attributed to its electrolyte uptake tendency.

The R_{ct} values for bare Cu and Al were observed to be low which is attributed to the materialization of porous oxide layer on the metal surface (Table 1, T1a and T1b). This layer permits the continuous diffusion of hydroxide (OH^-) and chloride ions (Cl^-) towards the metal surface due to which we have observed low R_{ct} and high C_c values. Due to the existence of a WBPU barrier layer over the Cu and Al surface, the R_{ct} values of WBPU coated specimens are observed to be significantly up-surged than the bare Cu and Al. These R_{ct} values further increased significantly after the inclusion of PGZ nanocomposite in the WBPU. The observed R_{ct} values of specimens coated with 3.0% of PGZ in WBPU is much higher than that of the specimen coated with WBPU solution, exhibiting its excellent tendency to protect underlying metal from corrosion. The electrolyte uptake tendency of substrate coated with 3.0% PGZ is found to be lowest which is depicted by the low value of C_c.

The Bode's plots (Log |Z| vs Log Frequency) for the substrates coated with the 3.0% PGZ in WBPU show higher impedance values in the low-frequency region. This low frequency region represents the protective barrier characteristics of the coating materials via high impedance modulus (Sathiyanarayanan et al., 1992; Chowdhury and Kant, 2018). The phase angle values for PGZ coated substrates (Figs. 7b and 8b) are observed to be less than WBPU coated substrates, these low values in the low frequency regime are attributed to the compactness of protective barrier layer (Chowdhury and Kant, 2018).

The prevention of diffusion of ions from the aggressive electrolyte is one of the major requirements from a coating material during its exposure to the harsh environments. Table 1, T1a and T1b depict the impedance response of coated substrates exposed to 3.5% NaCl for a persistent period of 30 days. The C_c values are observed to be significantly lower for 3.0% PGZ in WBPU coated substrates exhibiting lower tendency of electrolyte uptake which resulted in the development of highly protective surface barrier coating that further provided significant corrosion shielding even after a prolonged period of exposure to aggressive electrolyte. A similar trend for impedance response was observed for all concentrations of PGZ coating systems. The corresponding Nyquist and Bode's plots for Cu and Al for an exposure time of up to 30 days are given as supplementary information in fig. S1(i-vi) and S2 (i-vi) respectively.

3.6. Potentiodynamic polarization study

Potentiodynamic polarization study is a commonly used electrochemical technique for evaluating the corrosion behavior of materials. In the case of coated substrates, the technique is used to investigate the protective properties of the coating. The study involves applying a potential to the coated metal and measuring the resulting current as the potential is swept. The potential is swept between a cathodic and anodic region to determine the corrosion potential and the polarization resistance of the coating.

The data obtained from the potentiodynamic polarization study can provide information on the effectiveness of the coating in preventing corrosion. A higher polarization resistance indicates better protection against corrosion, while a lower resistance suggests the coating may be less effective

Table 2
Corrosion current densities of bare metals (Cu and Al), WBPU coated metals and 3.0% PGZ in WBPU coated metals specimen exposed to 3.5% NaCl Solution.

Composition (%)	Corrosion Current Density (I_{corr}) ($\mu A\ cm^{-2}$)*10^{-3}					
	After 1 day	After 5 days	After 10 days	After 15 days	After 20 days	After 30 days
For Copper (Cu) Specimens						
Bare Cu	54074	148398	190341	1423763	7848594	15169095
WBPU	2227	2602	3051	4469	8344	11541
3.0% PGZ in WBPU	86	720	997	1022	1376	1819
For Aluminum (Al) Specimens						
Bare Al	8019	9309	12753	17132	18535	20970
WBPU	1029	1376	1708	1998	3638	5542
3.0% PGZ in WBPU	26	279	281	619	958	1904

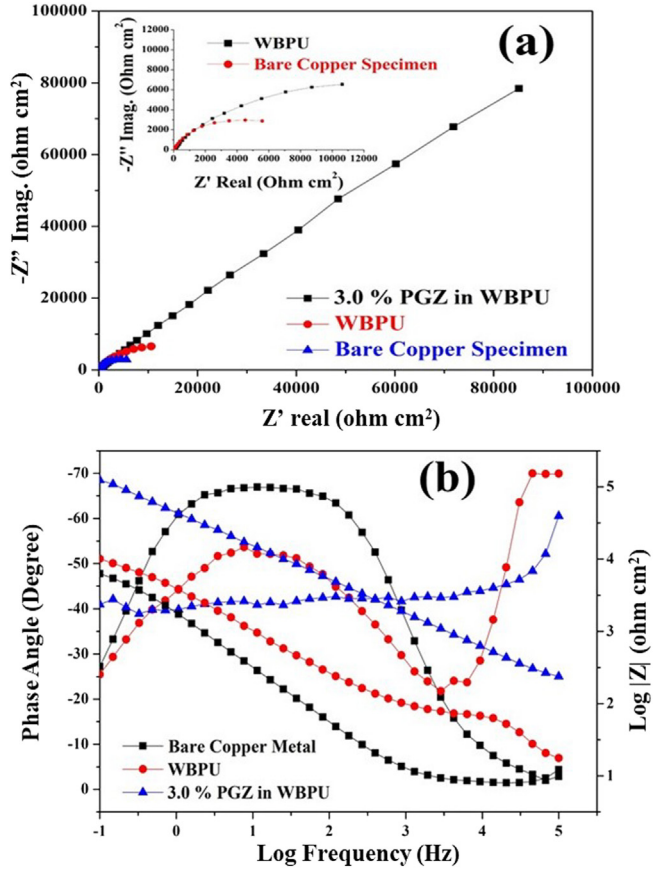

Fig. 7. Nyquist (a) and bode's (b) plots for bare Cu, WBPU coated Cu and 3.0% PGZ in WBPU coated Cu substrates after 1 day of exposure to 3.5% NaCl solution.

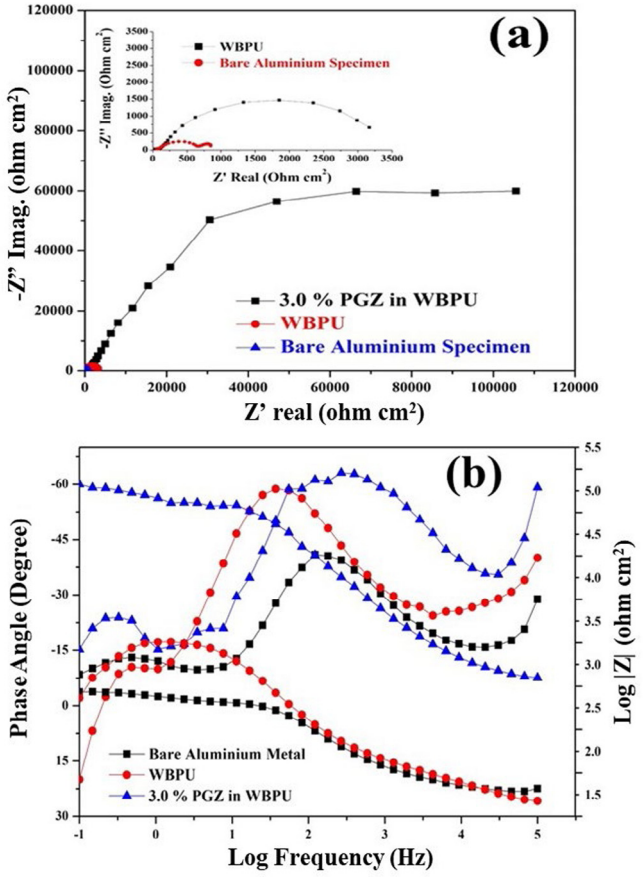

Fig. 8. Nyquist (a) and bode's (b) plots for bare Al, WBPUcoated Al and 3.0% PGZ in WBPU coated Al substrates after 1 day of exposure to 3.5% NaCl solution.

Figs. 9a and 9b show the polarization curves for bare and coated Cu and Al specimens after 1 day of exposure to aggressive neutral chloride solution. The corresponding Tafel parameters depicted from the polarization curves viz. corrosion potential (E_{corr}), corrosion current density (i_{corr}), anodic (β_a) and cathodic (β_c) slopes (Table 2, T2a and T2b). From the data, it can easily be inferred that the coated Cu and Al substrates demonstrated impressively lower i_{corr} and more positive E_{corr} values w.r.t. bare substrates, which is attributed to the development of highly stable passive film on the metal specimens encouraged by the coating material which further leads to high level of protection from the destructive force of corrosion. It can also be noted from Table 2 that the i_{corr} values of binder coated Cu and Al specimens are less than the specimens coated with 3.0 % PGZ in WBPU. This shows the enhanced fencing characteristic of PGZ-WBPU coatings under highly corrosive conditions (Christopher et al., 2016). The lower i_{corr} values attributed towards the formation of a highly effective shielding film on both the metal surface. These values suggest that the PGZ nanocomposite is optimally doped (Chaudhari and Patil, 2007) and is in sufficient concentration to show redox characteristics in the investigated systems.

For making a distinction among the various investigated coating systems (1.0% to 5.0% loadings of PGZ nanocomposite in WBPU), the Tafel polarization plots for coated Cu and Al specimens were also recorded and illustrated in figure S3(i-vi) and S4(i-vi) respectively. The i_{corr} values for PGZ coatings viz. 1.0%, 2.0%, 4.0% and 5.0% are observed to be higher as compared to specimens coated with 3.0% PGZ in WBPU (Table T2a and T2b). The shift of E_{corr} towards negative regime is due to the existence of dynamic corrosion reactions at the coating-metal interface (Christopher et al., 2016). The interfacial bonding between coating and metal has been degraded with time due

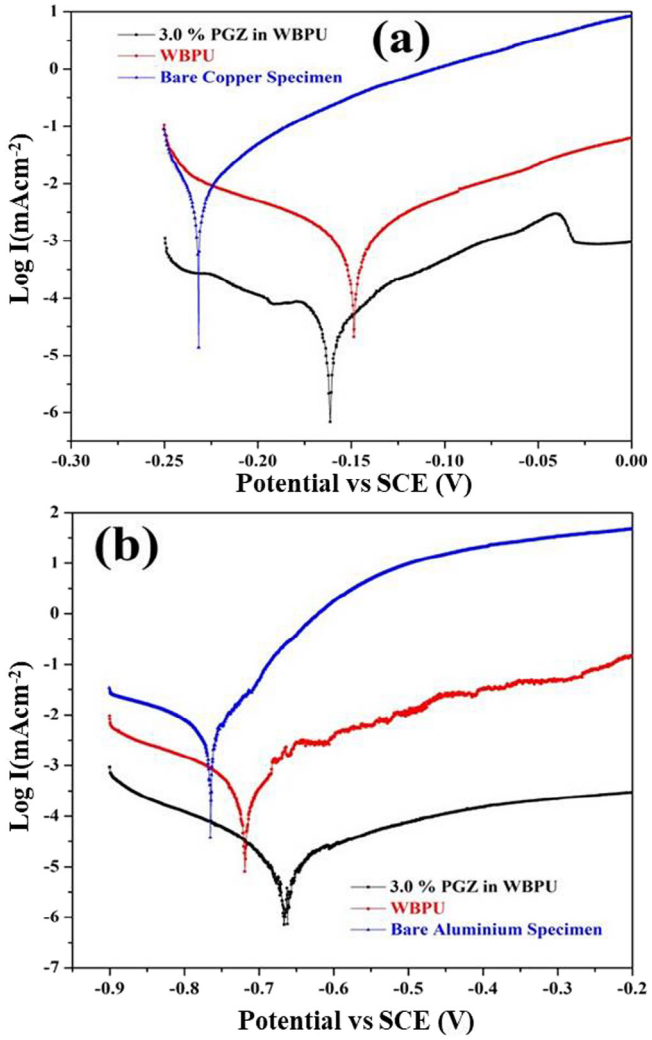

Fig. 9. Tafel polarization curves for Cu (a) and Al (b): bare, coated with WBPU and coated with 3.0% PGZ in WBPU solution after an exposure period of 1 day to 3.5% NaCl solution.

to the unremitting diffusion of aggressive ions penetrating the interface as shown by the data time studies. The earlier studies have proved that the higher loading concentrations of composite materials affect negatively on the coating film via making it more porous and susceptible towards formation of defects and diffusion of aggressive ions from the electrolyte whereas the lower loading concentration provides adequate corrosion resistance to the underlying substrate (Kumar et al., 2013; Choi et al., 1999; Luo et al., 2014).

The main component of PGZ nanocomposite is PEDOT, its electrode potential magnitude is higher than the active metals and their alloys. This vital characteristic assists PEDOT to interact with these metal substrates and to modify their corrosion characteristics. At the metal–polymer interface, PEDOT assist in the formation of stable passive oxide layer via redox reactions (Christopher et al., 2016). The large surface area of GO sheet aided in the retardation of diffusion of aggressive chloride ions from the electrolyte towards the metal substrates. ZrO_2 nanoparticles enhanced the overall compactness and provided stability to the coating material.

In general, the i_{corr} values of all the investigated coating formulations upsurge sluggishly with the increase of exposure time to the neutral chloride solution. The much noble E_{corr} values and lower i_{corr} values distinctively demonstrated the significantly higher anti-corrosion characteristic of the PGZ coating that eventually augmented the overall corrosion resistance of WBPU coatings in which it is doped with various concentrations.

4. Conclusions

The PGZ nanocomposite was successfully fabricated by in-situ oxidative chemical polymerization method and characterized via state of the art techniques. WBPU coatings doped with PGZ nanocomposite were successfully applied on to the Cu and Al substrates. The impedance parameters illustrated the significant reduction in charge transfer resistance (R_{ct}) values of all the PGZ coated specimens of both the metals. The potentiodynamic polarization studies indicate significantly lower i_{corr} values for all the Cu and Al specimens coated with various loadings (wt. %) of PGZ in a binder solution. Among all the coating variants the best results were delivered by 3.0% of PGZ nanocomposite coating system. This coating (3.0% PGZ in WBPU) has shown superior corrosion protection even after prolonged exposure of up to 30 days to aggressive sodium chloride solution.

Declaration of competing interest

The authors declare that they have no known competing financial interests or personal relationships which have, or could be perceived to have, influenced the work reported in this article.

Data availability

The raw/processed data required to reproduce these findings cannot be shared at this time as the data also forms part of an ongoing study.

Acknowledgments

This research work was supported by Korea Institute of Energy Technology Evaluation and Planning (KETEP) (20162010103990) grant funded by the Korean Ministry of Trade, Industry and Energy.

Appendix A. Supplementary data

Supplementary material related to this article can be found online at https://doi.org/10.1016/j.rsurfi.2023.100139.Figure S1 to S5, table T1 and T2 are provided as supplementary information.

References

Armelin, E., et al., 2009. Surf. Coat. Technol. 203, 3763–3769.
Bai, X., et al., 2015. Corros. Sci. 95, 110–116.
Bastos, A.C., Ferreira, M.G.S., Simões, A.M., 2005. Prog. Org. Coat. 52 (4), 339–350.
Beccaria, A.M., Chiaruttini, L., 1999. Corros. Sci. 41, 885–899.
Brusic, V., Angelopoulas, M., Graham, T., 1997. J. Electrochem. Soc. 144 (2), 436.
Cano, M., Khan, U., Sainsbury, T., O'Neill, A., Wang, Z., McGovern, I.T., Maser, W.K., Benito, A.M., Coleman, J.N., 2013. Carbon 52, 363.
Cascalheira, A.C., Aeiyach, S., Lacaze, P.C., Abrantes, L.M., 2003. Electrochim. Acta 48, 2523.
Cecchetto, L., Delabouglise, D., Petit, Jean-Pierre, 2007. Electrochim. Acta 52 (11), 3485–3492.
Chaudhari, S., Patil, P., 2007. Electrochim. Acta 53 (2), 927–933.
Choi, J.W., Han, M.G., Kim, S.Y., Oh, S.G., Im, S.S., 2004. Synth. Met. 141, 293.
Choi, H.J., Kim, J.W., To, K., 1999. Polymer 40 (8), 2163–2166.
Chowdhury, N.R., Kant, R., 2018. Electrochim. Acta 281, 445–458.
Christopher, G., et al., 2016. Prog. Org. Coat. 99, 91–102.
da Silva, J.E. Pereira, de Torresi, S.I. Córdoba, Torresi, R.M., 2005. Corros. Sci. 47, 811–822.
Dutta, K., De, S.K., 2007. Phys. Lett. A 361 (1–2), 141–145.
Eda, G., Chhowalla, M., 2010. Adv. Mater. 22, 2392.
Fateh, A., Aliofkhazraei, M., Rezvanian, A.R., 2017. Arab. J. Chem. http://dx.doi.org/10.1016/j.arabjc.2017.05.021.
Fenelon, A.M., Breslin, C.B., 2002. Electrochim. Acta 47, 4467.
Hasanov, R., Bilgiç, S., 2009. Prog. Org. coat. 64, 435–445.
Hasanov, R., Bilgiç, S., Gece, G., 2011. J. Solid State Electrochem. 15, 1063–1070.
Kalendová, A., Veselý, D., Kohl, M., Stejskal, J., 2015. Prog. Org. coat. 78, 1–20.
Kear, G., Barker, B.D., Stokes, K.R., Walsh, F.C., 2005. Corros. Sci. 47, 1694–1705.
Kendig, M.W., Davenport, A.J., Isaacs, H.S., 1993. Corros. Sci. 34 (1), 41–49.

Khasim, S., Pasha, A., Badi, N., Lakshmi, M., Al-Ghamdi, S.A., AL-Aoh, H.A., 2021. J. Polym. Environ. 29, 612–623.
Kinsella, Whelan M., Carbonell, L., Ho, H.M., Maex, K., 2003. Microelectron. Eng. 70, 551–557.
Kowalczyk, K., Luczka, K., 2015. J. Coat. Technol. Res. 12 (1), 153–165.
Kuila, T., Mishra, A.K., Khanra, P., Kim, N.H., Lee, J.H., 2013. Nanoscale 5 (1), 52–71.
Kumar, S.A., et al., 2013. Polym. Int. 62 (8), 1192–1201.
Lamaka, S.V., Zheludkevich, M.L., Yasakau, K.A., Montemor, M.F., Ferreira, M.G.S., 2007. Electrochim. Acta 52, 7231–7247.
Lerf, A., He, H., Foster, M., Klinowski, J., 1998. J. Phys. Chem. B 102, 4477.
Li, S., Teague, Mary T., Doll, Gary L., Schindelholz, Eric J., Cong, H., 2018. Corros. Sci. 141, 243–254.
Liu, Y., Liu, S.Y., Li, S.Y., Zhang, J.J., Liu, J.A., Han, Z.W., Ren, L.Q., 2015. Corros. Sci. 94, 190–196.
Liu, W., Xu, Q.J., Han, J., Chen, X.H., Min, Y.L., 2016. Corros. Sci. 110, 105–113.
Lokesh, K.S., De Keersmaecker, M., Elia, A., Depla, D., Dubruel, P., Vandenabeele, P., Vlierberghe, S.V., Adriaens, A., 2012. Corros. Sci. 62, 73–82.
Luo, Y., et al., 2014. J. Mater. Chem. C 2 (11), 1990–1994.
May, P., Khan, U., O'Neill, A., Coleman, J.N., 2012. J. Mater. Chem. 22, 1278.
Muller, D., et al., 2016. Coatings 6, 36.
Nguyen-Tri, P., et al., 2018. Int. J. Corros. http://dx.doi.org/10.1155/2018/4749501.
Padawer, G.E., Beecher, N., 1970. Polym. Eng. Sci. 10, 185.
Putz, K.W., Compton, O.C., Palmeri, M.J., Nguyen, S.T., Brinson, L.C., 2010. Adv. Funct. Mater. 20, 3322.
Rattana, T., et al., 2012. Procedia Eng. 32, 759–764.
Rickerby, J., Steinke, J.H.G., 2002. Chem. Rev. 102, 1525–1550.
Sathiyanarayanan, S., et al., 1992. Corros. Sci. 33 (12), 1831–1841.
Shi, X., Dalal, N.S., 1994. Environ. Health Perspect. 102 (Suppl. 3), 231–236.
Shi, X., et al., 2009. Surf. Coat. Technol. 204 (3), 237–245.
Simões, A.M., Battocchi, D., Tallman, D.E., Bierwagen, G.P., 2007. Corros. Sci. 49 (10), 3838–3849.
Stankiewicz, A., et al., 2013. J. Mater. Sci. 48, 8041–8051.
Stankovich, S., Dikin, D.A., Dommett, G.H.B., Kohlhass, K.M., Zimney, E.J., Stach, E.A., Piner, R.D., Nguyen, S.T., Ruoff, R.S., 2006. Nature 442, 282.
Steppan, J.J., Roth, J.A., Hall, L.C., Jeannotte, D.A., Carbone, S.P., 1987. J. Electrochem. Soc. 134, 175.
Tan, C.K., Blackwood, D.J., 2003. Corros. Sci. 45, 545–557.
Xhanari, K., Finšgar, M., 2016. Arab. J. Chem. http://dx.doi.org/10.1016/j.arabjc.2016.08.009.
Zhao, J., Xia, L., Sehgal, A., Lu, D., McCreery, R.L., Frankel, G.S., 2001. Surf. Coat. Technol. 140, 51–57.